

Detecting Exceptional Point through Dynamics in Non-Hermitian Systems

Keshav Das Agarwal, Tanoy Kanti Konar, Leela Ganesh Chandra Lakkaraju, Aditi Sen(De)
Harish-Chandra Research Institute, HBNI, Chhatnag Road, Jhunsi, Allahabad 211 019, India

Non-Hermitian rotation-time reversal (\mathcal{RT})-symmetric spin models possess two distinct phases, the unbroken phase in which the entire spectrum is real and the broken phase which contains complex eigenspectra, thereby indicating a transition point, referred to as an exceptional point. We report that the dynamical quantities, namely short and long time average of Loschmidt echo which is the overlap between the initial and the final states, and the corresponding rate function, can faithfully predict the exceptional point known in the equilibrium scenario. In particular, when the initial state is prepared in the unbroken phase and the system is either quenched to the broken or unbroken phase, we analytically demonstrate that the rate function and the average Loschmidt echo can distinguish between the quench occurred in the broken or the unbroken phase for the nearest-neighbor XY model with uniform and alternating magnetic fields, thereby indicating the exceptional point. Furthermore, we exhibit that such quantities are capable of identifying the exceptional point even in models like the non-Hermitian XYZ model with magnetic field which can only be solved numerically.

I. INTRODUCTION

Non-Hermitian systems have recently attracted a lot of interest as a result of the intricate extension of quantum mechanics and the advancements made in quantum technologies, such as quantum sensing [1–3], quantum metrology [4], and state tomography [5]. The realization of perfect state transfer on \mathcal{PT} -symmetric network [6], and the observation of a quantum phase transition via maximal entanglement generation in a non-Hermitian system [7] which cannot be observed in its Hermitian counterparts make the study of non-Hermitian systems more intriguing. These non-Hermitian models exhibit a phase transition point, also known as an exceptional point (EP) [8, 9], where the eigenspectrum changes from real to imaginary. Importantly, EP in these systems have already been observed in optical setups, cold atom and cavity systems [10–13]. It also plays a crucial role in the study of open system dynamics in Liouvillian evolution, where adjusting the EP via the external Hamiltonian parameter helps to regularize the dynamics of the system, which, in turn, aids in the development of better thermal machines [14]. Therefore, identifying the transition point in a non-Hermitian system is crucial.

On the other hand, in quantum many-body systems, quantum phase transition (QPT) can show a signature of quantum properties [15], more specifically, the transition is driven due to quantum fluctuations at zero temperatures. It has also been discovered that during evolution, the behavior of the Loschmidt echo, which is the overlap between the initial and final states with time, may discriminate between two scenarios – in one, the quenching and the initial Hamiltonian are in separate phases, while in the other, they are in the same phase [16, 17]. The phenomenon is referred to as dynamical quantum phase transition (DQPT) [18–20] (cf. [21–23]) which was initially demonstrated using the quantum transverse Ising model. In this regard, several counter-intuitive results are also reported [24–27] which include non-uniformly spaced critical time in the XY model with uniform and alternate

magnetic fields, detection of phase boundary at finite temperature via long time average of Loschmidt echo [28], enhanced sensitivity in connection with quantum sensing [29], dynamical signature to disclose localization-delocalization transition in Aubry-André (AA) model [30]. Since there are only a few many-body Hamiltonian which can be diagonalized analytically, the observation of DQPT can also be a potential method to predict a possible QPT at equilibrium. Moreover, DQPT has already been captured in laboratories with physical systems like cold atoms and trapped ions [31, 32]. Notice that in all these investigations, the Hamiltonian used for the initial state and the evolution is Hermitian.

Due to the inherent complexities involved in the dynamics of non-Hermitian systems such as the interpretation of inner product, the study of the evolution of the non-Hermitian systems under sudden quench is limited [33–35]. However, some recent studies that address this issue arrive at some interesting results like distinguishing localization regime of \mathcal{PT} -symmetric AA model by longtime survival probability [36], and the consequence of non-Hermitian gapless phase on DQPT in p -wave superconductor [37–39].

In this work, we explore the evolution of pseudo-Hermitian rotation-time reversal (\mathcal{RT})-symmetric model when the initial state is prepared in the unbroken phase. The prominent examples of \mathcal{RT} -symmetric Hamiltonian include XY model with imaginary anisotropy parameter in presence of uniform and alternating transverse magnetic field, referred to as iXY and $iATXY$ models respectively, having coterminus exceptional points. Using the technique employed for the corresponding Hermitian models [40, 41], both the models can be mapped to spinless fermions [42, 43] and hence their dynamics can be studied analytically both for finite and infinite system sizes. We demonstrate that the rate function derived from Loschmidt echo along with the averaged value of the Loschmidt echo in a short and long time can determine whether the quenching is performed across the EP or not. In particular, from the unbroken to broken

quench, the rate function increases monotonically and saturates to a nonvanishing value while at the sudden quench to the unbroken phase, the rate function oscillates at a very low value. It is interesting to note that the biorthogonalization technique should be employed to calculate the fidelity between the initial and final states, allowing one to correctly define the dual of a vector for the non-Hermitian model. We illustrate that the non-analytic behavior in the derivative of the long-time averaged rate function correctly indicates the exceptional point obtained in the static situation both for the *iXY* and the *iATXY* models.

In addition to the exactly solvable models, we deal with the *iXYZ* model having short and long range interactions which can be studied via exact diagonalization. In these non-Hermitian models also, we reveal that dynamical quantifiers, both Loschmidt echo and short-time averaged of it, are able to accurately identify the exceptional point in equilibrium, thereby mimicking equilibrium physics from the study of non-equilibrium.

This paper is organized as follows. In Sec. II, we introduce the quantities that we use to analyze DQPT for short as well as long time while we describe different non-hermitian Hamiltonians in Sec. III. The exceptional points for these Hamiltonians and bi-orthogonalization procedure to match usual quantum mechanics is explained in Sec. IV. Analytical computation of Loschmidt echo and the behavior of rate function for the *iXY* and *iATXY* models which detect EP are presented in Sec. V. In Sec. VI, we extend the scenario to capture exceptional point through DQPT for system like *iXYZ* with long range interaction which can only be solved numerically. Finally, we draw conclusion of our findings in Sec. VII.

II. DYNAMICAL QUANTIFIERS

More popularly, dynamical quantum phase transitions have been quantified by the non-analytic behavior of a distance function of the evolved and initial states [44], called Loschmidt echo [17, 45, 46]. It is defined as

$$\mathcal{L}(t) = \frac{|\langle \Psi(0) | \Psi(t) \rangle|^2}{\langle \Psi(t) | \Psi(t) \rangle}, \quad (1)$$

where $|\Psi(0)\rangle$ is the initial state of the Hamiltonian while $|\Psi(t)\rangle$ represents the evolved state after a quench. Typically, the initial state is considered to be the ground state of the Hamiltonian, $H(\lambda)$ at $t = 0$, corresponding to a certain phase while the evolution occurs due to a sudden change of parameters in the Hamiltonian at $t > 0$, $H(\lambda')$ which may or may not belong to the same phase as $H(\lambda)$, thereby indicating a quantum phase transition between λ and λ' . We are interested in the situation when $|\Psi(t)\rangle$ is orthogonal to $|\Psi(0)\rangle$, thereby arriving to vanishing $\mathcal{L}(t)$. More vividly, one can capture this feature by determining

Loschmidt rate, which is defined as

$$\lambda(t) = -\lim_{N \rightarrow \infty} \frac{1}{N} \ln \mathcal{L}(t) \quad (2)$$

where N is the system size, and $N \rightarrow \infty$ is taken for the thermodynamic limit. Note that the rate function is an analogue of free energy as it is the logarithm of a function that resembles the partition function when the corresponding inverse temperature is replaced with the imaginary time. The corresponding non-analyticities, known as Fisher zeros, indicate the crossing of a phase boundary and hence, equilibrium phase transition can be replicated using non-equilibrium dynamics successfully in Hermitian systems [16] (for exceptional cases, see [25–28])

In this work, we will employ these quantifiers, both $\mathcal{L}(t)$ and $\lambda(t)$, to study non-Hermitian systems. Specifically, instead of quantum critical points, our aim is to detect the exceptional point which distinguishes between broken and unbroken phases in non-Hermitian systems from the dynamics. Precisely, the initial state is chosen from the unbroken phase (entire spectrum of the Hamiltonian is real), while the system is quenched either to the broken (some eigenvalues have non-zero imaginary component) or the unbroken phase and we investigate $\mathcal{L}(t)$ or $\lambda(t)$ to predict whether the system has crossed exceptional point or not.

As mentioned before, although in many situations Loschmidt rate can identify equilibrium phase transition successfully, there are Hamiltonian including quantum *XY*-model with uniform and alternating magnetic field for which the quantifiers fail [25–28]. To avoid such discrepancy, in case of Hermitian systems, time averaged Loschmidt rate and Loschmidt echo are used [47].

To determine exceptional points through dynamics for non-Hermitian Hamiltonian, we adopt four figures of merits, Loschmidt echo, rate function and other two averages of the dynamical quantities, where the averaging is either performed in the transient or in the steady state regimes. Mathematically, the averaged quantities are defined as

$$\begin{aligned} \eta^T &= -\frac{1}{N} \ln \left(\frac{1}{\tau_0} \int_0^{\tau_0} \mathcal{L}(t) dt \right), \\ \eta^S &= -\frac{1}{N} \ln \left(\lim_{\tau \rightarrow \infty} \frac{1}{\tau - \tau_1} \int_{\tau_1}^{\tau} \mathcal{L}(t) dt \right), \end{aligned} \quad (3)$$

where τ_0 and τ_1 describe the end of transient time and beginning time of the steady state regime respectively. It has been shown [47] that η^S can be used to distinguish between phases, thereby confirming the existence of quantum critical points in different Hermitian models. We propose here that η^S (averaged Loschmidt echo) is capable to differentiate broken and unbroken phases in the steady state domain while η^T can perform the same job in transient regime and is better for models with finite system sizes, especially for the models which can only be solved numerically.

III. \mathcal{RT} -SYMMETRY AND NON-HERMITIAN QUENCH

Non-Hermiticity in spin models can be introduced either by imaginary magnetic fields [48] or by considering imaginary anisotropy parameter in the interactions [49] that can reveal several novel features [50]. In this regard, rotational-time (\mathcal{RT}) symmetry was found to be one of the facets through which the spectrum can be made real in a non-Hermitian interacting spin systems.

The rotation operator rotates each spin by angle $\frac{\pi}{2}$ about the z -axis, i.e., $\mathcal{R} = \exp\left[-i\frac{\pi}{4}\sum_i^N \sigma_i^z\right]$ while the time reversal operator, \mathcal{T} , which is the complex conjugation in finite dimensional system is an anti-linear operator, i.e., $\mathcal{T}\mathcal{R}\mathcal{T} = -i$. Although Hamiltonian commutes with the \mathcal{RT} operator (while the Hamiltonian does not commute with the \mathcal{R} and the \mathcal{T} operators individually), they may not share the common eigenvectors due to the anti-linearity of the time reversal operator \mathcal{T} . However, when they do share the eigenspectrum, the Hamiltonian has the real eigenvalues and is in the unbroken phase. Hence, by varying parameter of the Hamiltonian, we can traverse in between the broken and the unbroken regions.

A. Non-Hermitian iXY Hamiltonian

The rotation operator \mathcal{R} essentially maps Pauli matrix σ^x to σ^y and vice versa while σ^z remains unchanged as the rotation is about the same. Thus, in order to look for the models that are endowed with \mathcal{RT} -symmetry, we should look for the cases that have complex conjugated coefficients from the interactions or the magnetic fields in the x and y directions.

Following that, we investigate a variety of possible models. Replacing the anisotropy parameter, γ by $i\gamma$ in the prototypical quantum XY model with nearest neighbor interactions in a transverse magnetic field, we obtain iXY model which possess \mathcal{RT} -symmetry and it reads as

$$\bar{H}_{iXY} = \sum_{l=1}^N \frac{J}{4} [(1+i\gamma)\sigma_l^x\sigma_{l+1}^x + (1-i\gamma)\sigma_l^y\sigma_{l+1}^y] - \frac{h'}{2}\sigma_l^z,$$

with the periodic boundary condition, $\sigma_{N+1}^i \equiv \sigma_1^i$ ($\{i \in x, y, z\}$), J and h' being the coupling constant and the strength of magnetic field respectively. To make the analysis dimensionless, we set $\frac{h'}{J} = h$.

Applying the same recipe used in the Hermitian XY models [40, 41], one can diagonalize the iXY model via Jordan-Wigner transformation which converts the Pauli matrices to spinless fermions, followed by the Fourier transform which maps it to a momentum space and finally the Bogoliubov transformation leading to a spectrum of the Hamiltonian (see Appendix. A). Therefore, Hamiltonian reduces to the momentum space in block-diagonal form in which each block can be represented as

$$\begin{aligned} \bar{H}_{iXY}^p &= \begin{bmatrix} h & -\gamma \sin \phi_p & 0 & 0 \\ \gamma \sin \phi_p & 2 \cos \phi_p - h & 0 & 0 \\ 0 & 0 & \cos \phi_p & 0 \\ 0 & 0 & 0 & \cos \phi_p \end{bmatrix} \\ &= \begin{bmatrix} 1 & 0 \\ 0 & 0 \end{bmatrix} \otimes H_{iXY}^p + \cos \phi_p I, \end{aligned} \quad (4)$$

where $H_{iXY}^p = \begin{bmatrix} h - \cos \phi_p & -\gamma \sin \phi_p \\ \gamma \sin \phi_p & \cos \phi_p - h \end{bmatrix}$ is traceless and I is the 4×4 identity matrix. The above diagonalization can help to investigate several features of this model, both for finite and infinite sized systems in static as well as in dynamics. We find the relevant quantities of interest during which we perform summation over all momenta p . In the thermodynamic limit, i.e., as $N \rightarrow \infty$, the summation over ϕ_p for finite N transforms to the integral with $\phi_p \in (0, \pi]$.

B. Non-Hermitian $iATXY$ model

Another prominent quantum spin model which can be analytically solved by using the similar prescription as in the iXY model is the non-Hermitian nearest-neighbor XY model with both uniform and alternating magnetic fields in the transverse directions, referred to as $iATXY$ model [43]. The governing Hamiltonian reads as

$$\begin{aligned} \bar{H}_{iATXY} &= \sum_{l=1}^N \frac{J}{4} [(1+i\gamma)\sigma_l^x\sigma_{l+1}^x + (1-i\gamma)\sigma_l^y\sigma_{l+1}^y] \\ &\quad - \frac{h' + (-1)^l h'_a}{2} \sigma_l^z \end{aligned} \quad (5)$$

with $\frac{h' \pm h'_a}{J} = h \pm h_a$ being the strength of the magnetic field at odd and even sites respectively with periodic boundary conditions. In terms of spin ladder operators, it reduces to

$$\begin{aligned} H_{iATXY} &= \bar{H}_{iATXY} - \frac{Nh}{2} = \sum_{l=1}^N \left[\frac{i\gamma}{2} (\sigma_l^+ \sigma_{l+1}^+ + \sigma_l^- \sigma_{l+1}^-) \right. \\ &\quad \left. + \frac{1}{2} (\sigma_l^+ \sigma_{l+1}^- + \sigma_l^- \sigma_{l+1}^+) - (h + (-1)^l h_a) \sigma_l^+ \sigma_l^- \right] \end{aligned} \quad (6)$$

Unlike the iXY model, the modified Jordan-Wigner transformation [43, 51] changes the one-dimensional model to two-component Fermi gas based on even and odd sites, followed by the Fourier transform. Therefore, the Hamiltonian in Eq. (6) transforms to a direct product of 16×16 matrices, and each matrix is written as direct sum of $2, 4, 4$ and 6 dimensional blocks. For all momentum p , the lowest energy state is found in the following 4×4 block, i.e., with $\phi_p \in [-\pi/2, \pi/2]$ in the

thermodynamic limit, we have H_{iATXY}^p as

$$\begin{bmatrix} h + \cos \phi_p & -\gamma \sin \phi_p & 0 & -h_a \\ \gamma \sin \phi_p & -h - \cos \phi_p & h_a & 0 \\ 0 & h_a & \cos \phi_p - h & -\gamma \sin \phi_p \\ -h_a & 0 & \gamma \sin \phi_p & h - \cos \phi_p \end{bmatrix}. \quad (7)$$

C. Non-Hermitian $iXYZ$ models: Short and Long range interactions

Upto now, all the non-Hermitian models that we discussed are analytically diagonalizable. We will use those for studying dynamical states, especially by changing the magnetic fields. Apart from these models, we also consider model which can only be solved by numerical means or approximate methods. Specifically, we deal with $iXYZ$ models having \mathcal{RT} -symmetry with short range (SR) and long range (LR) interactions, given respectively by

$$\begin{aligned} \bar{H}_{iXYZ} = \sum_{l=1}^N \frac{J}{4} & [(1+i\gamma)\sigma_l^x \sigma_{l+1}^x + (1-i\gamma)\sigma_l^y \sigma_{l+1}^y \\ & + \Delta \sigma_l^z \sigma_{l+1}^z] - \sum_{l=1}^N \frac{h'}{2} \sigma_l^z, \end{aligned} \quad (8)$$

and

$$\begin{aligned} \bar{H}_{iXYZ}^{LR} = \sum_{l,m} \frac{J_{lm}}{4} & [(1+i\gamma)\sigma_l^x \sigma_m^x + (1-i\gamma)\sigma_l^y \sigma_m^y \\ & + \Delta \sigma_l^z \sigma_m^z] - \sum_{l=1}^N \frac{h'}{2} \sigma_l^z, \end{aligned} \quad (9)$$

with periodic boundary condition, Δ being the strength of interactions in the z -direction, $J_{lm} = \frac{J}{|l-m|^\alpha}$ with α being the falling-rate of the interactions with distance between the spins, and $\frac{h'}{J} = h$ being the strength of the magnetic field. In the Hermitian cases, the former model can be realized in photonic systems [52] while the latter models are found in experiments with trapped ions [53] and superconducting circuits. Moreover, the long range Hermitian models typically reveal novel characteristics like violation of area-law [54, 55], fast transfer of states [56] which cannot be found in models having SR interactions.

IV. EXCEPTIONAL POINTS AND BI-ORTHOGONALIZATION

A defining property of non-Hermitian Hamiltonian is the existence of exceptional points. This is the point which distinguishes two regions having real and complex energy spectra, corresponding to the unbroken and the

broken phases respectively. We first discuss the procedure to find and calculate the exceptional points of all the models considered in this work.

Since in the case of non-Hermitian Hamiltonian the eigenvectors are, in general, non-orthogonal, we then define an inner product with respect to a metric, known as bi-orthogonalization, in such a way that the eigenvectors become orthogonal. We will discuss this procedure in order to make the results more comprehensive.

A. Unbroken to broken transition: Exceptional points

After finding the energy spectrum of the Hamiltonian which can be obtained either by analytical means in the iXY and the $iATXY$ models or by numerical simulations, one needs to solve for two equations, namely, $\frac{\partial \epsilon_p(h_{ep})}{\partial p} = 0$ and $\epsilon_p(h_{ep}) = 0$ to find the momentum value p at which the energy vanishes with ϵ_p being the energy spectrum in terms of momentum basis and h_{ep} being the exceptional point. An exceptional point can be obtained by solving these two equations simultaneously which collectively imply that when the ground state energy becomes zero, the system undergoes a transition from broken to unbroken phase.

By solving Eq. (4), we obtain the eigenvalues of the iXY Hamiltonian as

$$\epsilon_p^\mp = \mp \sqrt{(h - \cos \phi_p)^2 - \gamma^2 \sin^2 \phi_p}, \quad (10)$$

where the corresponding eigenvectors are $|v_p^-\rangle$ and $|v_p^+\rangle$ respectively. They are written in the columns of a matrix, P_p , as

$$P_p = \frac{1}{\sqrt{2\epsilon_p}} \begin{bmatrix} \sqrt{h - \cos \phi_p - \epsilon_p} & -\sqrt{h - \cos \phi_p + \epsilon_p} \\ -\sqrt{h - \cos \phi_p + \epsilon_p} & \sqrt{h - \cos \phi_p - \epsilon_p} \end{bmatrix} \quad (11)$$

where $\epsilon_p = |\epsilon_p^\mp|$. Following the procedure outlined above, one can show that when $h > h_{ep}^{iXY}$ with $h_{ep}^{iXY} = \sqrt{1 + \gamma^2}$ being the exceptional point, all the eigenvalues are real, i.e., $\epsilon_p^\mp \in \mathbb{R} \forall p$, which represents the unbroken phase, since the eigenvectors shown above also diagonalize the \mathcal{RT} operator. When $h < h_{ep}^{iXY}$, the eigenvectors of H_{iXY} and \mathcal{RT} operator are different, thereby leading the spectrum being complex. Even though $[\bar{H}_{iXY}, \mathcal{RT}] = 0$, they do not share the same set of eigenvectors due to the anti-linear nature of \mathcal{RT} . Also, in the broken phase, the Hamiltonian becomes defective, i.e., the geometric multiplicity is less than the algebraic multiplicity of the eigenvalues.

Following the similar prescription, in the case of $iATXY$ model, the exceptional point can also be derived [43]. The H_{iATXY}^p model, as described in Eq. (7), has

eigenvalues

$$\begin{aligned} \bar{\epsilon}_p^{\pm(\pm)} &= \pm [h^2 + h_a^2 + \cos^2 \phi_p - \gamma^2 \sin^2 \phi_p \\ &\quad \pm 2\sqrt{h^2 h_a^2 + h^2 \cos^2 \phi_p - h_a^2 \gamma^2 \sin^2 \phi_p}]^{1/2}. \end{aligned} \quad (12)$$

Among four eigenvalues, we can easily argue that the exceptional point, $h_{ep}^{iATXY} = \sqrt{1 + h_a^2 + \gamma^2}$ can be found from $\bar{\epsilon}_p^{\pm(-)}$ i.e., when $h > h_{ep}^{iATXY}$, $\bar{\epsilon}_p^{\pm(\pm)} \in \mathbb{R} \forall p$.

It has recently been shown by some of us that the exceptional points in the \mathcal{RT} -symmetric Hamiltonian are closely related to the factorization surface where the ground state of the Hamiltonian is fully product with vanishing entanglement of the corresponding Hermitian model [43]. This prescription allows one to find the exceptional point even for the systems which have no analytical solution. For instance, the above connection leads to the exceptional point as $h_{ep}^{iXYZ} = \sqrt{(1 + \Delta)^2 + \gamma^2}$ for the $iXYZ$ model in Eqs. (8) which does not have an analytical solution and can be confirmed via numerical diagonalization. This procedure also suggests that in presence of long range interactions of the form of Eq. (9), the exceptional point is $h_{ep}^{iXYZ_{LR}} = \sqrt{(1 + \Delta)^2 + \gamma^2} \sum_{j=1}^{N/2} \frac{1}{j^\alpha}$.

B. Bi-orthogonalization metric

Eigenvectors, which represent states of the systems need to be mutually orthonormal in order to distinguish between states faithfully and maintain the probability between zero and one. In case of Hermitian systems, the observables are represented by Hermitian operators, for which, the states are orthonormal by default.

In order to check orthonormality between two vectors, one has the inner product metric in the Hilbert space where the vectors reside. Specifically, the way in which the dual vector is defined while finding the inner product ensures orthogonality. In case of Hermitian quantum mechanics, the dual is the transpose of a vector after complex conjugation and orthogonality is automatically maintained amongst eigenvectors. It is more subtle in case of non-Hermitian systems [57].

Depending on the Hamiltonian, we must define a metric. Note first that the eigenvectors of the iXY model as shown in P_p in Eq. (11) of a non-Hermitian matrix are non-orthogonal in the usual Euclidean norm. In this situation, bi-orthogonalization [58] can, in general, be performed for pseudo-Hermitian systems having linearly independent and complete set of eigenvectors. In particular, we define a non-singular metric operator, $\hat{\Theta}$ which connects the left eigenvectors to the right eigenvectors for each eigenvalue, i.e., for all the vectors $|\psi\rangle$, $\langle\psi|\hat{\Theta}$ becomes its dual. This makes the eigensystem of the pseudo-Hermitian operators H , bi-orthogonal. The metric operator $\hat{\Theta}$ should be Hermitian and satisfy $H^\dagger \hat{\Theta} = \hat{\Theta} H$.

We make the trivial choice of metric operators as $\hat{\Theta} = (P^{-1})^\dagger P^{-1}$, where P is the matrix with columns

as the eigenvectors. This shows that P^{-1} can be treated as the invertible Dyson map [59]. It allows us to treat the pseudo-Hermitian system as Hermitian in the metric space where non-orthogonal (in the Euclidean sense) basis vectors form a complete basis. Note that the matrix P is invertible only in the unbroken phases, where the eigenspace is non-defective.

For our analysis, we obtain the eigenspectrum of pseudo-Hermitian \mathcal{RT} -symmetric Hamiltonian H , and obtain $\hat{\Theta}$ from the eigenvector matrix P of the corresponding H . This is used for bi-orthogonalizing the Hamiltonian in the corresponding model, which makes the initial Hamiltonian Hermitian although during the dynamics, the quenched Hamiltonian still remains non-Hermitian. As shown in the succeeding section, the entire formalism enables us to study the non-equilibrium physics of the non-Hermitian models, in a similar fashion as was done for Hermitian models in the literature [33].

V. DISTINGUISHING EXCEPTIONAL POINT VIA LOSCHMIDT RATE IN iXY AND $iATXY$ MODELS

Let us now focus on the response of Loschmidt echo after quenching the Hamiltonian in different phases across exceptional point. In particular, the initial state is chosen to be the ground state of the Hamiltonian, H^0 in the unbroken phase. The reason for the choice of the initial state is two-fold — firstly, it is unambiguous to identify the ground state in the unbroken phase, when the spectrum is real; secondly, the P matrix which contains the eigenvectors is of full-rank and has a well-defined inverse, thereby allowing us to easily compute the expectation values meaningfully.

A. Dynamics of iXY model

To present our results for the iXY model, let us first fix the stage. After the preparation of the initial state corresponding to the Hamiltonian, $(H^0)_{iXY}^p$, we evolve the system according to the Hamiltonian, $(H^1)_{iXY}^p$, by varying the external magnetic field, h . As mentioned before, the parameters involved in the Hamiltonian for the initial state is fixed in the unbroken phase while the Hamiltonian corresponding to the evolution operator is chosen from both the broken and the unbroken phases, thereby producing the dynamical state which is the main interest of the paper. Specifically, the initial magnetic field is adopted such that $h_0 > h_{ep}^{iXY}$ while at $t > 0$, the quench is performed by changing the external magnetic field to h_1 . Notice that the corresponding eigenvalues are given by $\epsilon_p^{0,1} = \sqrt{(h_{0,1} - \cos \phi_p)^2 - \gamma^2 \sin^2 \phi_p}$, where ϵ_p^0 and ϵ_p^1 are the eigenvalues obtained from the initial and the quenched Hamiltonian momentum blocks. In the eigenspace of $(H^0)_{iXY}^p$ (given in Eq. (11) with

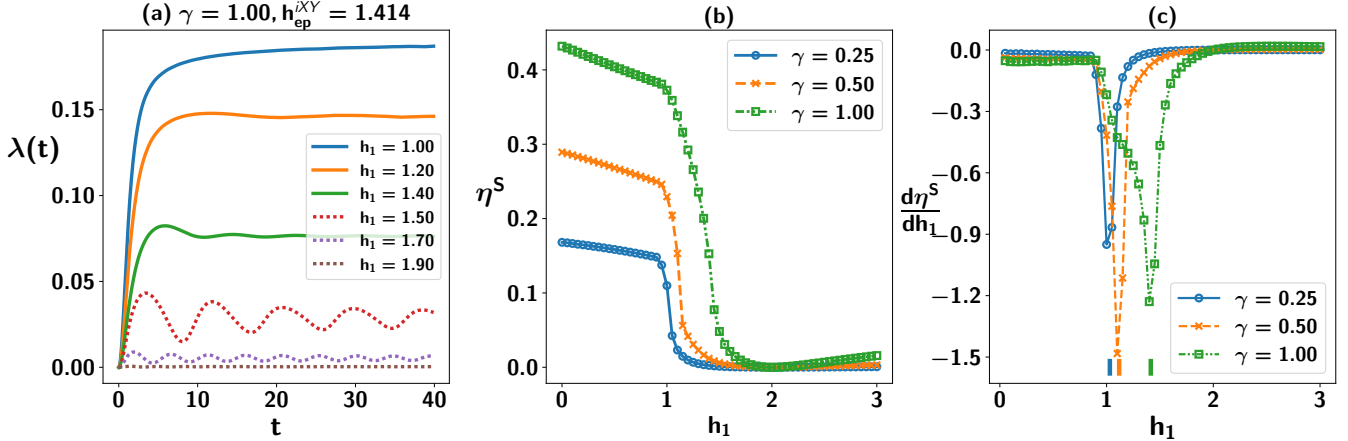


FIG. 1. **Detecting exceptional point in the iXY model.** The ground state is taken at $h_0 = 2.0 > h_{ep}^{iXY} = 1.414$ for all γ as the initial state for the evolution. (a) Rate function (ordinate) defined in Eq. (2) with respect to time (t) (abscissa) for the iXY Hamiltonian in Eq. (4) with $\gamma = 1.0$. The sudden quench is performed by changing the magnetic fields to h_1 mentioned in legends. Solid lines represent quenching from unbroken to broken phase while dotted lines are for the quenching in the same phase. (b) Distinguishing between the broken and unbroken phases using η^S (vertical axis) defined in Eq. (3) against h_1 (horizontal axis) for different values of γ . For calculating η^S , the averaging is performed during $t \in [20, 200]$. (c) Derivative of η^S with respect to h_1 (vertical axis) is plotted with post-quenched magnetic fields, (h_1) (horizontal axis). The non-analyticity of $\frac{d\eta^S}{dh_1}$ signals the EP marked underneath by a vertical bar which are obtained analytically for equilibrium. We take the system size, $N = 1200$ for different non-Hermiticity parameters, γ . All the axes are dimensionless.

the magnetic field strength h_0), which is, equivalently, bi-orthogonalizing the vectors, the initial Hamiltonian would be diagonal, i.e., $(H^0)_{iXY}^p = \begin{bmatrix} -\epsilon_p^0 & 0 \\ 0 & \epsilon_p^0 \end{bmatrix}$, and the final Hamiltonian, with which we perform the quench, written in the same basis as $(H^0)_{iXY}^p$ reads as

$$(H^1)_{iXY}^p = \frac{1}{\epsilon_p^0} \begin{bmatrix} -\delta_p & \omega_p \\ -\omega_p & \delta_p \end{bmatrix}, \quad (13)$$

where $\delta_p = (h_0 - \cos \phi_p)(h_1 - \cos \phi_p) - \gamma^2 \sin^2 \phi_p$ and $\omega_p = \gamma(h_1 - h_0) \sin \phi_p$. Note that $(H^1)_{iXY}^p$ is still non-Hermitian. Therefore, the time-evolution operator, in this case, can be represented as [33],

$$U_{iXY}^p(t) = e^{-i(H^1)_{iXY}^p t} = \cos \epsilon_p^1 t \mathbb{I} - i \frac{\sin \epsilon_p^1 t}{\epsilon_p^1} (H^1)_{iXY}^p. \quad (14)$$

Since the initial Hamiltonian is diagonal, its ground state is $|\psi_p(0)\rangle = [1 \ 0]^T$ and the evolved state can take the form as

$$|\psi_p(t)\rangle = U_{iXY}^p(t) |\psi_p(0)\rangle = \begin{bmatrix} \cos \epsilon_p^1 t - i \frac{\delta_p \sin \epsilon_p^1 t}{\epsilon_p^0 \epsilon_p^1} \\ i \frac{\omega_p \sin \epsilon_p^1 t}{\epsilon_p^0 \epsilon_p^1} \end{bmatrix} := \begin{bmatrix} a_p(t) \\ b_p(t) \end{bmatrix}. \quad (15)$$

Due to non-Hermiticity, we normalize the dynamical state which leads to Loschmidt echo in Eq. (1). Finally, for the iXY model, the expression for the Loschmidt echo

reads as

$$\mathcal{L}(t) = \prod_p \mathcal{L}_p(h_0, h_1, \gamma, t) = \prod_p \left(\frac{|a_p(t)|^2}{|a_p(t)|^2 + |b_p(t)|^2} \right). \quad (16)$$

We now exhibit that by analyzing $\mathcal{L}(t)$, one can distinguish between broken and unbroken phases, thereby identifying exceptional point. A general matrix representation of a non-Hermitian Hamiltonian H can be written in Jordan canonical form \mathcal{J} , with respect to some basis (columns of matrix \mathcal{S}), such that $H = \mathcal{S} \mathcal{J} \mathcal{S}^{-1}$. These are decomposed in Jordan blocks, $\mathcal{J} = \bigoplus_l \mathcal{J}_l$ with complex or real eigenvalues λ_l . When the order of degeneracy in the eigenvalue is equal to the eigenspace dimension, Jordan blocks are diagonal and give the eigenvectors in the unbroken phase, where the Hamiltonian is non-defective. The evolved state by the action of the evolution operator $U(t) = \bigoplus_l U_l(t)$ on $|\Psi(0)\rangle$ is given by

$$|\Psi(t)\rangle = U(t)|\Psi(0)\rangle = \mathcal{S} e^{-i\mathcal{J}t} \mathcal{S}^{-1} |\Psi(0)\rangle. \quad (17)$$

In the unbroken phase, the Jordan form of each $(H^1)_{iXY}^p$ is diagonal with real eigenvalues $\mp \epsilon_p^1$ and complete eigenbasis, \mathcal{S}_p . Therefore, in the eigenbasis \mathcal{S}_p , the initial state reads as $|\psi_p(0)\rangle = c_1 |\mathcal{S}_1^p\rangle + c_2 |\mathcal{S}_2^p\rangle$, where $|\mathcal{S}_{1,2}^p\rangle$ are the first and the second columns of \mathcal{S}^p respectively, and $\langle \psi_p(0) | = c_1^* \langle \mathcal{S}_1^{-1} | + c_2^* \langle \mathcal{S}_2^{-1} |$ where $\langle \mathcal{S}_{1,2}^{-1} |$ represent the first and the second row of $(\mathcal{S}^p)^{-1}$, with $|c_1|^2 + |c_2|^2 = 1$. After quenching in the unbroken phase, the Jordan form is diagonal and the Loschmidt echo reduces to

$$\begin{aligned} \mathcal{L}_p^U(t) &= | |c_1|^2 e^{i\epsilon_p^1 t} + |c_2|^2 e^{-i\epsilon_p^1 t} |^2 \\ &= \cos^2 \epsilon_p^1 t + (|c_1|^2 - |c_2|^2)^2 \sin^2 \epsilon_p^1 t \end{aligned} \quad (18)$$

where $\pm \epsilon_p^1$ are the real eigenvalues of quenching Hamiltonian. It indicates that $\mathcal{L}_p^{\mathcal{U}}(t)$ is oscillatory for all t and for all momentum p in the unbroken phase. We will show that this is indeed the case (see Fig. 1(a) when $h > h_{ep}^{iXY}$).

On the other hand, when we quench in the broken phase, the Hamiltonian becomes defective with the vanishing degenerate eigenvalue for certain critical momentum ϕ_{p^c} . The defective 2×2 traceless Hamiltonian, H_{p^c} , in the Jordan canonical form \mathcal{J}_{p^c} becomes

$$\mathcal{J}_{p^c} = \begin{bmatrix} 0 & 1 \\ 0 & 0 \end{bmatrix} \implies e^{-i\mathcal{J}_{p^c}t} = \begin{bmatrix} 0 & -it \\ 0 & 0 \end{bmatrix}. \quad (19)$$

The Loschmidt echo in Eq. (1) in this situation reduces to

$$\mathcal{L}_{p^c}^{\mathcal{B}}(t) = \frac{|1 - itc_2c_1^*|^2}{|c_1|^2 + t^2|c_2|^2 - itc_1^*c_2 + itc_2^*c_1}, \quad (20)$$

where both the numerator and the denominator are polynomial in t . With increasing t , the numerator is dominated by the term, $t^2|c_1|^2|c_2|^2$ and the denominator by $t^2|c_2|^2$. Therefore, $\lim_{t \rightarrow \infty} \mathcal{L}_{p^c}^{\mathcal{B}}(t) = |c_1|^2 < 1$ as the initial and the final Hamiltonian are non-commuting and do not share the basis of the Jordan form. It implies that at the beginning of the evolution, the Loschmidt echo decays if the quenching Hamiltonian is defective. Such analysis demonstrates the following.

The difference in behavior of a dynamical quantity, namely $\mathcal{L}(t)$, in two different phases, broken and unbroken, is capable to predict the existence of exceptional point in equilibrium, without the explicit computation of eigenvalues.

In the case of *iATXY* model, exactly solving the Hamiltonian, H_{iATXY}^p and finding the eigenvector for arbitrary parameters is cumbersome. We numerically diagonalize Eq. (7) to obtain the corresponding metric and vectors in the momentum space which enables us to compute quantities for this model with a high system-size or in the thermodynamic limit. We then compute the corresponding figures of merit as discussed above. By numerically computing $\mathcal{L}_p(t)$ with 4×4 matrices, we calculate the rate function $\lambda(t)$, defined in Eq. (2). For both *iXY* ($h_a = 0$) and *iATXY* models, the rate function in the thermodynamic limit reduces to

$$\lambda(h_0, h_1, \gamma, h_a, t) = - \int \frac{d\phi_p}{2\pi} \ln(\mathcal{L}_p(h_0, h_1, \gamma, h_a, t)), \quad (21)$$

which is a function of all the parameters involved in the system.

Analysis of rate function and averaged Loschmidt echos. Let us now analyze the profile of the rate function, $\lambda(t)$ or the Loschmidt echo, $\mathcal{L}(t)$ for different systems starting from the ground state of H^0 . We mainly concentrate on two scenarios – (1) unbroken to broken quench and (2) unbroken to unbroken quench. Notice that in the *iXY* and the *iATXY* models, we look at

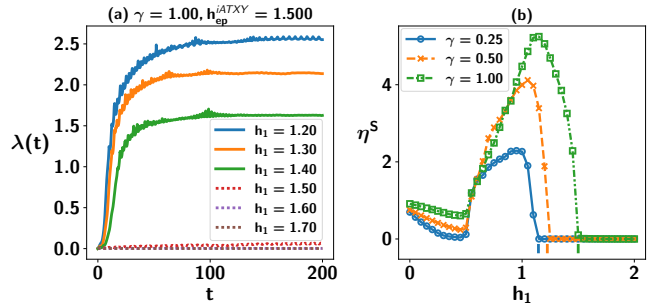


FIG. 2. **Identifying EP of the *iATXY* model.** The ground state at $h_0 = 3.0 > h_{ep}^{iATXY}$ being taken as the initial state for all γ . We fix $h_a = 0.5$ for our analysis. (a) Rate function, $\lambda(t)$, (y -axis) as a function of t (x -axis) for $\gamma = 1.0$. (b) Rate of average Loschmidt echo (η^S) (ordinate) in the steady state regime against the post-quench magnetic field (h_1) (abscissa). From the analysis, we find that the steady state is reached at $t = 100$, which is used to compute η^S during $100 \leq t \leq 500$. Here $N = 100$ for different non-Hermiticity parameter, γ . The corresponding actual exceptional points are marked underneath by a vertical bar. All the axes are dimensionless.

the behavior of $\lambda(t)$, since the Loschmidt echo $\mathcal{L}(t)$ becomes exponentially small with increasing system size N , thereby exponentially increasing Hilbert space dimension. On the other hand, we examine the behavior of Loschmidt echo, $\mathcal{L}(t)$ for the *iXYZ* models in the next section where the study is based on the numerical diagonalization.

Unbroken to broken quench. Since we are interested to locate the exceptional point of a non-Hermitian model, we first consider the situation where the initial state is prepared in the unbroken phase and the system is quenched to the broken phase of the model.

In the *iXY* model, the rate function shows a steep rise in the transient regime (0 to $\tau_0 = 10$) (solid lines in Fig. 1(a) by taking the ground state at $h_0 = 2.0 > h_{ep}^{iXY}$ as the initial state) when $h_1 < h_{ep}$ and saturates to a non-vanishing value near the exceptional point in the steady state domain (from $\tau_1 = 20 > \tau_0$ to ∞). In Fig. 1(a), the anisotropy parameter is chosen to be unity, i.e., $\gamma = 1.0$, with the corresponding exceptional point at $h_{ep}^{iXY} = \sqrt{2}$. We perform the convergence test for the numerical integration of the rate function as in Eq. (21), find that $\lambda(t)$ converges at $N = 1000$ in the *iXY* model and hence we choose $N = 1200$ for illustration in Fig. 1.

On the other hand, for a fixed γ , η^S decreases uniformly with increasing h_1 (by a step of 0.05), till $h_1 = 1$, and then it decreases as a convex function, until the exceptional point as depicted in Fig. 1(b). The change of curvature from concavity to convexity in η^S leads to a sharp kink in $\frac{d\eta^S}{dh_1}$ at the exceptional point which is shown in Fig. 1(c) by a small vertical bars above the horizontal axis as obtained analytically in the equilibrium case. It clearly displays that the kink in dynamics is in a good agreement with the exact value obtained in static situa-

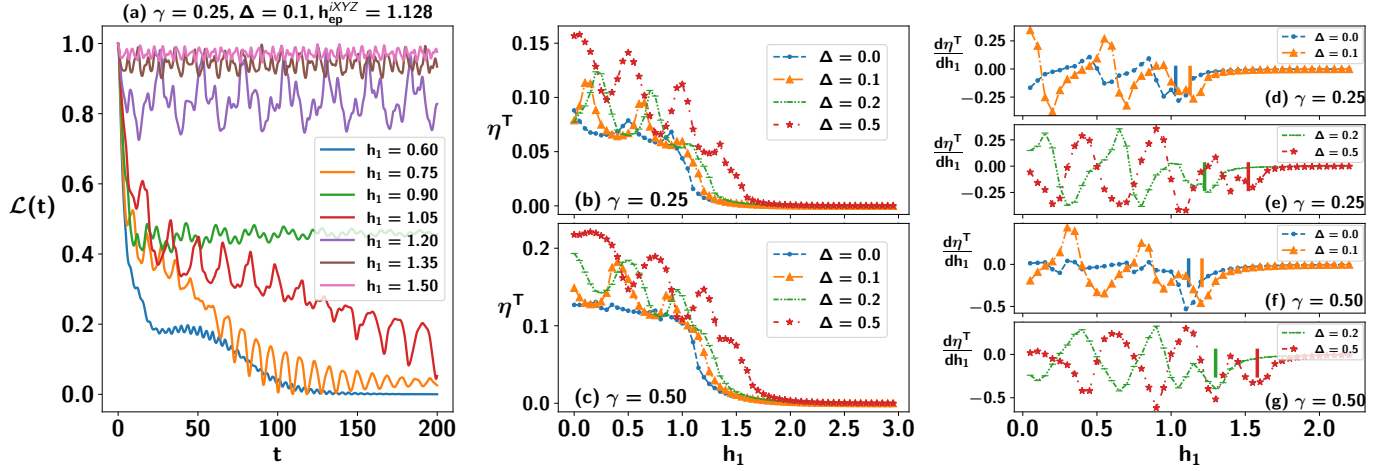


FIG. 3. **Evolution of the nearest-neighbor $iXYZ$ model** with the magnetic field $h_0 = 3.0 > h_{ep}^{iXYZ}$ in which the initial state is prepared, for different Δ and γ . (a) Loschmidt echo, $\mathcal{L}(t)$, (ordinate) with respect to time (t) (abscissa), for $\Delta = 0.1$ and $\gamma = 0.25$ and quenching in the corresponding broken and unbroken phases. The steady state dynamics shows irregularity which can be due to finite size. (b) Short-time average of Loschmidt echo, η^T (ordinate), vs post-quenched magnetic field, h_1 (abscissa) for various γ and Δ . The transient regime is taken to be $t = 0$ to $t = 30$. (c) Behavior of $\frac{d\eta^T}{dh_1}$ (vertical axis) with respect to h_1 (horizontal axis). Here $N = 12$. The corresponding exceptional points obtained analytically are marked by a vertical bar. All the axes are dimensionless.

tion.

The similar pattern emerges for the $iATXY$ model. Specifically, for $\gamma = 1.0$ and with $h_a = 0.5$, $h_{ep}^{iATXY} = 1.5$, and when the initial state is prepared at $h_0 = 2.0 > h_{ep}^{iATXY}$, we observe the similar monotonic increase of $\lambda(t)$ with t in the initial duration of the dynamics while it converges to a positive value after a certain time (see Fig. 2 (a)). Interestingly, we find that the convergence occurs in this case with $N = 80$ which is much lower than the iXY model and hence we carry out our investigation with $N = 100$ in Fig. 2. Unlike the iXY model, the steady state value, η_S , is not monotonic with h_1 in the quench of the $iATXY$ broken phase, irrespective of the anisotropy and h_a as seen in Fig. 2(b), and decreases sharply as h_1 approaches the exceptional point, thereby discriminating unbroken phase from the broken one through the dynamics. The investigations exhibit that the prediction of the exceptional point made by the dynamical quantities matches with the exact exceptional point found in the static case.

Unbroken to unbroken quench. Let us now move to a different picture in which the parameters of the Hamiltonian in the evolution operator are chosen from the unbroken phase.

In the iXY model, when $h_1 > h_{ep}^{iXY}$, we observe that the rate function shows oscillatory behavior, with oscillations being dying out as the quench parameter h_1 is farther away from h_{ep} (see dotted lines in Fig. 1(a)) while in case of $iATXY$ model, $\lambda(t)$ is oscillating with very small amplitude as depicted in Fig. 2(a). It is clear that for the iXY model, η^S which does decrease initially and then increases slowly remains concave in the

unbroken phase. The similar feature can also be observed from the behavior of $\frac{d\eta^S}{dh_1}$ which keeps on increasing in the unbroken phase, as shown in Fig. 1(c). In contrast, η^S remains very close to 0 in the unbroken phase for the $iATXY$ model (see Fig. 2(b)).

VI. DISTINGUISHING BETWEEN BROKEN AND UNBROKEN PHASES FROM DYNAMICS VIA EXACT DIAGONALIZATION

Let us now check whether the prediction made in the preceding section with the exactly solvable models also hold for models which cannot be solved analytically. To demonstrate that, we deal with the $iXYZ$ models having both short and long range interactions given in Eqs. (8) and (9).

A. $iXYZ$ models with short and long range interactions

To investigate \mathcal{RT} -symmetric $iXYZ$ models, we employ exact diagonalization to find the corresponding ground state which is taken as the initial state and find the metric. Since we require the entire spectrum to define the metric of the Hamiltonian and we further want to study the dynamics, we cannot go beyond a certain system-sizes, which is $N = 12$. As discussed in the previous scenario, the initial state is prepared in the unbroken phase, i.e., $h_0 > h_{ep}$ of the corresponding model.

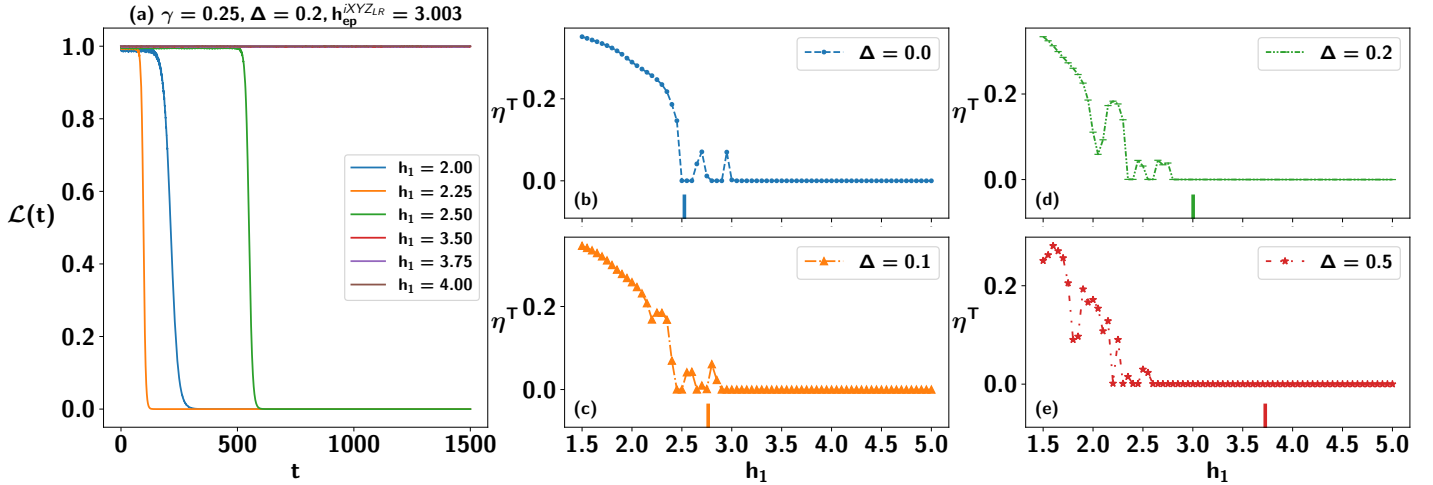


FIG. 4. **Predicting EP for the long range $iXYZ$** with decaying parameter $\alpha = 1$ and anisotropy parameter $\gamma = 0.25$. The ground state is taken at $h_0 = 5.0 > h_{ep} = 3.003$ which is in the unbroken phase for all values of Δ considered. (a) $\mathcal{L}(t)$ (ordinate) with respect to t (abscissa). The transient time behavior is steep when the parameters of the initial and final Hamiltonians are chosen from different phases. (b)-(e) η^T (ordinate) against the quenching magnetic field strength, h_1 , for different Δ . To calculate η^T , $\tau_0 = 800$ is taken. The corresponding expected exceptional points are marked by a vertical bar. All the axes are dimensionless.

Short range $iXYZ$ model. Let us first concentrate on the short range $iXYZ$ model. When the system is quenched to the broken phase, $\mathcal{L}(t)$ decreases sharply at the initial period of time and then oscillates with a fixed average value during the steady state dynamics. In contrast, when the evolution operator belongs to the unbroken phase, $\mathcal{L}(t)$ always oscillates with time having a fixed pattern and a fixed average value (see Fig. 3(a)).

The trends of $\mathcal{L}(t)$ possibly indicates that the Loschmidt echo in the transient regime, i.e., η^T carries the signature of exceptional point or the transition between broken and unbroken phase. As shown in Figs. 3(b) and 3(c), this is indeed the case. Specifically, for a fixed values of Δ and γ , we observe that *if η^T changes the curvature from concave to convex, we can definitely conclude that the initial Hamiltonian and the final Hamiltonian are chosen from different phases, i.e., it is quenched from the unbroken phase to a broken phase and vice versa.* In other words, at the exceptional point, $d\eta^T/dh_1$ surely exhibits a kink and such non-analytic behavior can also be seen if the evolution occurs due to the change from the unbroken phase to the broken phase.

Long range models. The situation is much more involved when we move to the model with long range interactions. The behavior of Loschmidt echo clearly distinguishes two scenarios. In particular, sharp decrease of $\mathcal{L}(t)$ in the transient regime determines the situation when the initial state is in the unbroken phase and the Hamiltonian is tuned to the broken phase at later time. Notice that unlike iXY , $iATXY$ and $iXYZ$ with short range interactions, the steep decay of $\mathcal{L}(t)$ occurs in large t . Such declining trend is absent when both the initial and the final Hamiltonian are chosen from the unbroken

phase. Therefore, η^T also carries the signature of phase transition occurred in equilibrium. As depicted in Fig. 4(b)-(e), we observe that when η^T stops fluctuating, we can conclude that the point is around the exceptional point. Specifically, we find that with the increase of Δ , the dip observed in η^T is moving far from the exceptional point. We believe that the conclusive determination of exceptional in the long range case is not possible due to finite size effect.

VII. CONCLUSION

By examining the time profile of the rate function and the long time average of the Loschmidt echo as a function of the post quench parameters, we analyzed the detection of an exceptional point (EP) in a non-hermitian systems. By using biorthogonalization method, we define a legitimate inner product in these systems. By preparing an initial state in the unbroken phase of a non-Hermitian nearest-neighbor XY model with alternating and uniform magnetic fields, sudden quench is performed either in the broken or in the unbroken phases. We observed that the trends of rate function clearly signals the transition point in these models. More precisely, long time behavior of Loschmidt echo with post quench parameter exhibits a sharp change around exceptional point known in the equilibrium, thereby predicting the EP.

We extended this dynamical strategy for recognizing EP in the nearest neighbor and long range $iXYZ$ model which can only be studied by numerical procedures. We observed that the average Loschmidt echo in the transient domain can clearly signal the existence of EP. Even

in presence of finite size effects. The successful detection method based on dynamics of quantum phase transition suggests the possibility of executing specific quantum information processing tasks in non-Hermitian models.

ACKNOWLEDGEMENTS

We acknowledge the support from Interdisciplinary Cyber Physical Systems (ICPS) program of the Department of Science and Technology (DST), India, Grant No.: DST/ICPS/QuST/Theme- 1/2019/23. We acknowledge the use of **QIClib** – a modern C++ library for general purpose quantum information processing and quantum computing (<https://titaschanda.github.io/QIClib>) and cluster computing facility at Harish-Chandra Research Institute.

[1] J. Wiersig, *Phys. Rev. A* **93**, 033809 (2016).

[2] W. Chen, S. Kaya Özdemir, G. Zhao, J. Wiersig, and L. Yang, *Nature* **548**, 192 (2017).

[3] H. Hodaei, A. U. Hassan, S. Wittek, H. Garcia-Gracia, R. El-Ganainy, D. N. Christodoulides, and M. Khajavikhan, *Nature* **548**, 187 (2017).

[4] C. Chen, L. Jin, and R.-B. Liu, *New Journal of Physics* **21**, 083002 (2019).

[5] M. Naghiloo, M. Abbasi, Y. N. Joglekar, and K. W. Murch, *Nature Physics* **15**, 1232 (2019).

[6] X. Z. Zhang, L. Jin, and Z. Song, *Phys. Rev. A* **85**, 012106 (2012).

[7] T. E. Lee, F. Reiter, and N. Moiseyev, *Phys. Rev. Lett.* **113**, 250401 (2014).

[8] C. M. Bender and S. Boettcher, *Phys. Rev. Lett.* **80**, 5243 (1998).

[9] C. M. Bender and D. J. Weir, *Journal of Physics A: Mathematical and Theoretical* **45**, 425303 (2012).

[10] M. Kreibich, J. Main, H. Cartarius, and G. Wunner, *Phys. Rev. A* **90**, 033630 (2014).

[11] M. Chitsazi, H. Li, F. M. Ellis, and T. Kottos, *Phys. Rev. Lett.* **119**, 093901 (2017).

[12] M.-A. Miri and A. Alù, *Science* **363**, eaar7709 (2019), <https://www.science.org/doi/pdf/10.1126/science.aar7709>.

[13] L. Pan, S. Chen, and X. Cui, *Phys. Rev. A* **99**, 063616 (2019).

[14] S. Khandelwal, N. Brunner, and G. Haack, *PRX Quantum* **2**, 040346 (2021).

[15] S. Sachdev, *Quantum Phase Transitions*, 2nd ed. (Cambridge University Press, 2011).

[16] M. Heyl, A. Polkovnikov, and S. Kehrein, *Phys. Rev. Lett.* **110**, 135704 (2013).

[17] M. Heyl, *Reports on Progress in Physics* **81**, 054001 (2018).

[18] M. Heyl, *Phys. Rev. Lett.* **115**, 140602 (2015).

[19] C. Karrasch and D. Schuricht, *Phys. Rev. B* **95**, 075143 (2017).

[20] S. Porta, F. Cavaliere, M. Sassetti, and N. Traverso Ziani, *Scientific Reports* **10**, 12766 (2020).

[21] K. Sengupta, S. Powell, and S. Sachdev, *Phys. Rev. A* **69**, 053616 (2004).

[22] A. Sen(De), U. Sen, and M. Lewenstein, *Phys. Rev. A* **72**, 052319 (2005).

[23] K. Sengupta, D. Sen, and S. Mondal, *Phys. Rev. Lett.* **100**, 077204 (2008).

[24] F. Andraschko and J. Sirker, *Phys. Rev. B* **89**, 125120 (2014).

[25] S. Vajna and B. Dóra, *Phys. Rev. B* **89**, 161105 (2014).

[26] V. Gurarie, *Phys. Rev. A* **100**, 031601 (2019).

[27] S. Halder, S. Roy, T. Chanda, A. Sen(De), and U. Sen, *Phys. Rev. B* **101**, 224304 (2020).

[28] P. Nandi, S. Bhattacharyya, and S. Dasgupta, *Phys. Rev. Lett.* **128**, 247201 (2022).

[29] Q. Guan and R. J. Lewis-Swan, *Phys. Rev. Res.* **3**, 033199 (2021).

[30] C. Yang, Y. Wang, P. Wang, X. Gao, and S. Chen, *Phys. Rev. B* **95**, 184201 (2017).

[31] P. Jurcevic, H. Shen, P. Hauke, C. Maier, T. Brydges, C. Hempel, B. P. Lanyon, M. Heyl, R. Blatt, and C. F. Roos, *Phys. Rev. Lett.* **119**, 080501 (2017).

[32] N. Fläschner, D. Vogel, M. Tarnowski, B. S. Rem, D.-S. Lühmann, M. Heyl, J. C. Budich, L. Mathey, K. Sengstock, and C. Weitenberg, *Nature Physics* **14**, 265 (2018).

[33] L. Zhou, Q.-h. Wang, H. Wang, and J. Gong, *Phys. Rev. A* **98**, 022129 (2018).

[34] L. Zhou and Q. Du, *New Journal of Physics* **23**, 063041 (2021).

[35] R. Hamazaki, *Nature Communications* **12**, 5108 (2021).

[36] Z. Xu and S. Chen, *Phys. Rev. A* **103**, 043325 (2021).

[37] L. Zhou, Q.-h. Wang, H. Wang, and J. Gong, *Phys. Rev. A* **98**, 022129 (2018).

[38] D. Mondal and T. Nag, *Phys. Rev. B* **106**, 054308 (2022).

[39] D. Mondal and T. Nag, “Finite temperature dynamical quantum phase transition in a non-hermitian system,” (2022).

[40] E. Barouch, B. M. McCoy, and M. Dresden, *Phys. Rev. A* **2**, 1075 (1970).

[41] E. Barouch and B. M. McCoy, *Phys. Rev. A* **3**, 786 (1971).

[42] X. Z. Zhang and Z. Song, *Phys. Rev. A* **87**, 012114 (2013).

[43] L. G. C. Lakkaraju and A. Sen(De), *Phys. Rev. A* **104**, 052222 (2021).

[44] R. Jozsa, *Journal of Modern Optics* **41**, 2315 (1994), <https://doi.org/10.1080/09500349414552171>.

[45] A. Silva, *Phys. Rev. Lett.* **101**, 120603 (2008).

[46] A. Peres, *Phys. Rev. A* **30**, 1610 (1984).

[47] B. Zhou, C. Yang, and S. Chen, *Phys. Rev. B* **100**, 184313 (2019).

[48] G. L. Giorgi, *Phys. Rev. B* **82**, 052404 (2010).

[49] X. Z. Zhang and Z. Song, *Phys. Rev. A* **87**, 012114 (2013).

[50] C. M. Bender, *Reports on Progress in Physics* **70**, 947 (2007).

- [51] S. Roy, T. Chanda, T. Das, D. Sadhukhan, A. Sen(De), and U. Sen, *Phys. Rev. B* **99**, 064422 (2019).
- [52] X.-s. Ma, B. Dakic, W. Naylor, A. Zeilinger, and P. Walther, *Nature Physics* **7**, 399 (2011).
- [53] A. Bermudez, L. Tagliacozzo, G. Sierra, and P. Richerme, *Phys. Rev. B* **95**, 024431 (2017).
- [54] A. E. B. Nielsen, G. Sierra, and J. I. Cirac, *Phys. Rev. A* **83**, 053807 (2011).
- [55] Z.-X. Gong, M. Foss-Feig, F. G. S. L. Brandão, and A. V. Gorshkov, *Phys. Rev. Lett.* **119**, 050501 (2017).
- [56] Z. Eldredge, Z.-X. Gong, J. T. Young, A. H. Moosavian, M. Foss-Feig, and A. V. Gorshkov, *Phys. Rev. Lett.* **119**, 170503 (2017).
- [57] D. C. Brody, *Journal of Physics A: Mathematical and Theoretical* **47**, 035305 (2013).
- [58] A. MOSTAFAZADEH, *International Journal of Geometric Methods in Modern Physics* **07**, 1191 (2010), <https://doi.org/10.1142/S0219887810004816>.
- [59] A. Fring and M. H. Y. Moussa, *Phys. Rev. A* **93**, 042114 (2016).

Appendix A: Diagonalization of iXY model

We now describe the diagonalization procedure for the Hamiltonian, given by

$$\bar{H}_{iXY} = \sum_{l=1}^N \frac{J}{4} [(1+i\gamma)\sigma_l^x \sigma_{l+1}^x + (1-i\gamma)\sigma_l^y \sigma_{l+1}^y] - \frac{h'}{2} \sigma_l^z.$$

Let us define the spin ladder operators, $(\sigma_l^+ \text{ and } \sigma_l^-)$, as

$$\sigma_l^+ = \frac{\sigma_l^x + i\sigma_l^y}{2}; \quad \sigma_l^- = \frac{\sigma_l^x - i\sigma_l^y}{2} \quad \forall l = 1, 2, \dots, N. \quad (\text{A1})$$

Thus the Hamiltonian in terms of raising and lowering operators reduces to

$$H_{iXY} = \bar{H}_{iXY}^{\mathcal{RT}} - \frac{Nh}{2} = \sum_{l=1}^N \left[\frac{i\gamma}{2} (\sigma_l^+ \sigma_{l+1}^+ + \sigma_l^- \sigma_{l+1}^-) + \frac{1}{2} (\sigma_l^+ \sigma_{l+1}^- + \sigma_l^- \sigma_{l+1}^+) - h \sigma_l^+ \sigma_l^- \right] \quad (\text{A2})$$

Let us now use the highly non-linear Jordan-Wigner transformation to represent H_{iXY} in terms of fermionic creation and annihilation operators, c_k^\dagger and c_k respec-

tively, with

$$c_k = e^{-i\pi \sum_{l=1}^{k-1} \sigma_l^+ \sigma_l^-} \sigma_k^-; \quad c_k^\dagger = \sigma_k^+ e^{i\pi \sum_{l=1}^{k-1} \sigma_l^+ \sigma_l^-}. \quad (\text{A3})$$

In the thermodynamic limit (i.e., $N \rightarrow \infty$), the boundary term would have infinitesimal contribution and hence ignoring the boundary term, we obtain

$$H_{iXY} = \sum_{k=1}^N \left[\frac{i\gamma}{2} (c_k^\dagger c_{k+1}^\dagger + c_k c_{k+1}) + \frac{1}{2} (c_k^\dagger c_{k+1} + c_k c_{k+1}^\dagger) - h c_k^\dagger c_k \right]. \quad (\text{A4})$$

We use the Fourier transform of the fermionic operators (because of the translation invariance), given by

$$a_p^\dagger = \frac{1}{\sqrt{N}} \sum_{k=1}^N e^{-ik\phi_p} c_k^\dagger; \quad a_p = \frac{1}{\sqrt{N}} \sum_{k=1}^N e^{ik\phi_p} c_k, \quad (\text{A5})$$

with $\phi_p = \frac{2\pi p}{N} \quad \forall p = \{-N/2, -N/2 + 1, \dots -1, 0, 1, \dots N/2 - 1, N/2\}$. Combining $\pm p$, H_{iXY} is decoupled in the basis, $\{|0\rangle, a_p^\dagger a_{-p}^\dagger |0\rangle, a_p^\dagger |0\rangle, a_{-p}^\dagger |0\rangle\}$, i.e.,

$$\bar{H}_{iXY} = \sum_{p=1}^{N/2} I \otimes I \otimes \dots \otimes \bar{H}_{iXY}^p \otimes \dots \otimes I, \quad (\text{A6})$$

with I being a 4×4 identity matrix and

$$\begin{aligned} \bar{H}_{iXY}^p &= \begin{bmatrix} h & -\gamma \sin \phi_p & 0 & 0 \\ \gamma \sin \phi_p & 2 \cos \phi_p - h & 0 & 0 \\ 0 & 0 & \cos \phi_p & 0 \\ 0 & 0 & 0 & \cos \phi_p \end{bmatrix} \\ &= \begin{bmatrix} 1 & 0 \\ 0 & 0 \end{bmatrix} \otimes H_{iXY}^p + \cos \phi_p I, \end{aligned} \quad (\text{A7})$$

where H_{iXY}^p is now a 2×2 traceless matrix represented as

$$H_{iXY}^p = \begin{bmatrix} h - \cos \phi_p & -\gamma \sin \phi_p \\ \gamma \sin \phi_p & \cos \phi_p - h \end{bmatrix}. \quad (\text{A8})$$